On the Performance of Cell-Free Massive MIMO in Ricean Fading (Invited Paper)

Published in:
IEEE International Conference on Signals, Systems, and Computers 2018 (IEEE ASILOMAR): Proceedings

Document Version:
Peer reviewed version

On the Performance of Cell–Free Massive MIMO in Ricean Fading

Hien Quoc Ngo*, Harsh Tataria*, Michail Matthaiou*, Shi Jin†, and Erik G. Larsson‡

*Institute of Electronics, Communications and Information Technology (ECIT), Queen's University Belfast, Belfast, U.K.
†National Mobile Communications Research Laboratory, Southeast University, Nanjing, P. R. China
‡Department of Electrical Engineering (ISY), Linköping University, Linköping, Sweden
e–mail: {hien.ngo, h.tataria, m.matthaiou}@qub.ac.uk, jinshi@seu.edu.cn, and erik.g.larsson@liu.se

Abstract—We consider an uplink time–division duplex cell–free massive multiple–input multiple–output (MIMO) system in which many user equipments (UEs) are simultaneously served by many access points (APs) via simple matched filtering processing. The propagation channel is modeled via the *Ricean* distribution, which includes a dominant line–of–sight component on top of diffuse scattering. The Ricean K–factor of each link *varies* with the UE location (relative to the locations of the APs). The system performance in terms of the spectral efficiency is investigated taking into account *imperfect* channel knowledge. Power and AP–weighting control is exploited to maximize the lowest spectral efficiency across all UEs. This optimization problem can be efficiently solved via the bisection method by solving a sequence of linear feasibility problems together with the generalized eigenvalue problem. We show that by optimally selecting the power control and AP–weighting coefficients, the per–UE throughput increases significantly. Furthermore, we propose an AP selection scheme to reduce the backhaul requirements in a cell–free massive MIMO system, with slight compromise in performance.

I. INTRODUCTION

In recent times, cell–free massive multiple–input multiple–output (MIMO) systems have stemmed from the amalgamation of contemporaneous massive MIMO with network MIMO systems [1]. In such a system, a large number of access points (APs) are geographically distributed, and connected to a central processing unit (CPU) via a fronthaul network. The APs coherently serve a smaller number of user equipments (UEs) within the same time–frequency resource. Since channel acquisition can be performed locally at each AP by leveraging the time–division duplex (TDD) reciprocity, cell–free massive MIMO systems can be considered as a scalable way to realize conventional network MIMO with joint processing [1]. By now, several studies have investigated the performance of cell–free systems with linear processing, imperfect channel estimation, and optimal resource allocation to maintain uniform service to each UE, see e.g., [1–5].

Despite these advancements, all of the above studies restrict the analyses and performance evaluations of cell–free systems to uncorrelated Rayleigh fading channels. This assumption is not realistic in practice, since the idea is to scale–up the number of APs relative to the total number of UEs in a given area. Consequently, the distance between APs and UEs decreases, leading to a significant increase in the probability of UEs experiencing dominant propagation paths from multiple APs. In such situations, line–of–sight (LOS) components dominate the channel impulse response, in addition to diffuse scattering.

This results in channel heterogeneity, since the LOS levels on multiple links are likely to vary depending on the UE location relative to the AP [6]. This does not only impact the resulting spectral efficiency of cell–free systems, but also has a direct consequence on the design of channel estimators, power control techniques, and AP selection schemes. Cell-free massive MIMO with Ricean fading was studied in [7]. The paper [7] focused on the performance comparison between minimum mean-square error (MMSE) and least-square estimators used in the uplink training phase, without any resource allocations, and under the assumption that the pilot sequences are assigned from a given set of orthogonal pilots. By contrast, in this work, we investigate the throughput of cell–free massive MIMO under Ricean fading channels with max-min power control and AP selection schemes. In addition, the pilot sequences in the training phase are assumed to be arbitrary.

Contributions. We evaluate the uplink spectral efficiency of cell–free massive MIMO with Ricean fading propagation. In doing so, we utilized a detailed model for the Ricean K–factor and link attenuation based on the probability of LOS and the link distance between a given AP and UE. We formulate and solve an optimization problem which selects power control and AP–weighting control coefficients in order to maximize the smallest spectral efficiency across all UEs. Precisely, we leverage the bisection method together with the generalized eigenvalue problem (described further in the text). Finally, an AP selection method is proposed to reduce the backhaul load, which shows a small spectral efficiency degradation.

II. SYSTEM MODEL

The uplink of cell–free massive MIMO is considered where the K UEs simultaneously transmit signals to M APs in the same frequency band. All APs and UEs are equipped with single–antennas, and are distributed in a large area. As in [1], all APs are connected to a CPU via perfect backhaul links.

A. Propagation Model

We consider Ricean fading channels, which consist of a dominant LOS component on top of a Rayleigh–distributed component modeling the scattered multipath. The channel from the m–th AP and to the k–th UE is modeled as

$$g_{mk} = \sqrt{\zeta_{mk}} \left(\sqrt{\frac{K_{mk}}{K_{mk}+1}} \bar{h}_{mk} + \sqrt{\frac{1}{K_{mk}+1}} \tilde{h}_{mk} \right), \quad (1)$$

where ζ_{mk} denotes the large–scale fading coefficient, K_{mk} is the Ricean K–factor, $\bar{h}_{mk}$ and $\tilde{h}_{mk}$ correspond to the LOS and non–LOS components, respectively. We assume that $\tilde{h}_{mk} \sim \mathcal{CN}(0,1)$, and $\bar{h}_{mk} = e^{j\omega_{mk}}$ where ω_{mk} denotes the *phase* of a random arrival angle. For simplicity, we denote

$$\bar{g}_{mk} = \sqrt{\zeta_{mk}}\sqrt{\frac{K_{mk}}{K_{mk}+1}}\bar{h}_{mk}, \ \beta_{mk} = \frac{\zeta_{mk}}{K_{mk}+1}.$$

Then, (1) can be rewritten as

$$g_{mk} = \bar{g}_{mk} + \sqrt{\beta_{mk}}\,\tilde{h}_{mk}. \tag{2}$$

We consider scenarios where users are fixed or move slowly, but there are movements of objects around them. In these scenarios, it is reasonable to assume that $\bar{g}_{mk}$ changes slowly with time, ad is known a priori. In addition, β_{mk} is also assumed to be known a priori.

B. Transmission Protocol

The transmission between the users to the APs is done in a TDD fashion. Precisely, each coherence interval is divided into *three* phases: uplink training, uplink data transmission, and downlink data transmission. Since our focus is on uplink transmission, we neglect the downlink data transmission phase.

1) Uplink Training: A part of the coherence interval of length τ_c symbols will be used for the uplink training phase to estimate the channels. During the training phase, all K UEs simultaneously send *pilot* sequences to the APs. Let τ_p be the length of the training duration, and $\sqrt{\tau_p}\boldsymbol{\varphi}_k \in \mathbb{C}^{\tau_p \times 1}$, where $\|\boldsymbol{\varphi}_k\|^2 = 1$, be the pilot sequence transmitted from the kth user, $k = 1, 2, \ldots, K$. Then, the $\tau_p \times 1$ received pilot vector at the m–th AP is

$$\mathbf{y}_{\mathrm{p},m} = \sqrt{\tau_p \rho_p}\sum_{k=1}^{K} g_{mk}\boldsymbol{\varphi}_k + \mathbf{w}_{\mathrm{p},m}, \tag{3}$$

where ρ_p represents the normalized signal–to–noise ratio (SNR) of each pilot symbol, and $\mathbf{w}_{\mathrm{p},m} \sim \mathcal{CN}(0, \mathbf{I}_{\tau_p})$ is the additive noise vector at the m–th AP. Denote by $\check{y}_{\mathrm{p},mk}$ the projection of $\mathbf{y}_{\mathrm{p},m}$ onto $\boldsymbol{\varphi}_k^H$, i.e. $\check{y}_{\mathrm{p},mk} = \boldsymbol{\varphi}_k^H \mathbf{y}_{\mathrm{p},m}$. Then, given $\check{y}_{\mathrm{p},mk}$, the MMSE estimate of g_{mk} is [8]

$$\hat{g}_{mk} = \bar{g}_{mk} + c_{mk}\left(\check{y}_{\mathrm{p},mk} - \bar{\check{y}}_{\mathrm{p},mk}\right), \tag{4}$$

where $\bar{\check{y}}_{\mathrm{p},mk} = \mathbb{E}\{\check{y}_{\mathrm{p},mk}\} = \sum_{k'=1}^{K}\sqrt{\tau_p\rho_p}\,\bar{g}_{mk'}\boldsymbol{\varphi}_k^H\boldsymbol{\varphi}_{k'}$, and

$$c_{mk} \triangleq \frac{\sqrt{\tau_p\rho_p}\,\beta_{mk}}{\tau_p\rho_p\sum_{k'=1}^{K}\beta_{mk'}\left|\boldsymbol{\varphi}_k^H\boldsymbol{\varphi}_{k'}\right|^2 + 1}.$$

Let $\epsilon_{mk} = g_{mk} - \hat{g}_{mk}$ be the channel estimation error. Then, from the MMSE estimation property, $\hat{g}_{mk}$ and ϵ_{mk} are uncorrelated. In addition, $\hat{g}_{mk} \sim \mathcal{CN}(\bar{g}_{mk}, \gamma_{mk})$, and $\epsilon_{mk} \sim \mathcal{CN}(0, \beta_{mk} - \gamma_{mk})$, where $\gamma_{mk} = \frac{\tau_p\rho_p\beta_{mk}^2}{\tau_p\rho_p\sum_{k'=1}^{K}\beta_{mk'}|\boldsymbol{\varphi}_k^H\boldsymbol{\varphi}_{k'}|^2+1}$.

C. Uplink Data Transmission

All K UEs simultaneously send their data to the APs. Denote by $\sqrt{\eta_k}q_k$, where $\mathbb{E}\{|q_k|^2\} = 1$ and $0 \leq \eta_k \leq 1$, the signal transmitted by the k–th UE. Here, q_k represents the data symbol and η_k represents the corresponding power control coefficient. Then, the m–th AP receives

$$y_{\mathrm{u},m} = \sqrt{\rho_u}\sum_{k=1}^{K} g_{mk}\sqrt{\eta_k}q_k + w_{\mathrm{u},m}, \tag{5}$$

where ρ_u is the normalized uplink SNR, and $w_{\mathrm{u},m} \sim \mathcal{CN}(0,1)$ denotes the additive noise at the m–th AP.

As in [3], to detect q_k, the received signal at the m–th AP will be first multiplied with the conjugate of its channel estimate, $\hat{g}_{mk}$, and an AP–weighting coefficient α_{mk}, and then the so–obtained quantity $\alpha_{mk}\hat{g}_{mk}^* y_{\mathrm{u},m}$ will be sent to the CPU via a backhaul network. The combined signal at the CPU is given by

$$r_{\mathrm{u},k} = \sum_{m=1}^{M} \alpha_{mk}\hat{g}_{mk}^* y_{\mathrm{u},m}. \tag{6}$$

Then, q_k is detected from $r_{\mathrm{u},k}$. Without loss of generality, we assume that $\sum_{m=1}^{M}|\alpha_{mk}|^2 \leq 1$.

Remark 1. In some cases, the signal received at the m–th AP contains very strong interference plus noise (relative to the desired signal). This may happen when the k–th UE is very far from the m–th AP or/and the other UEs are very close to this AP. For such cases, the AP–weighting coefficient α_{mk} should be small. Otherwise, the interference will be amplified, degrading the system performance. In Section IV, we discuss how to optimally select the values of α_{mk}.

III. SPECTRAL EFFICIENCY ANALYSIS

In this section, we provide a closed–form expression for the uplink spectral efficiency, via the use–and–forget bounding technique from [9]. With this technique, the spectral efficiency of the k–th UE is given by

$$R_k = \frac{\tau_c - \tau_p}{\tau_c}\log_2\left(1 + \frac{|\mathrm{DS}_k|^2}{\mathrm{BU}_k + \sum_{k'\neq k}^{K}\mathrm{UI}_{kk'} + \mathrm{AN}_k}\right). \tag{7}$$

where DS_k, BU_k, $\mathrm{UI}_{kk'}$, and AN_k represent the effects of the desired signal, the beamforming gain uncertainty, the interference from user k', and noise, respectively, given by

$$\mathrm{DS}_k \triangleq \sqrt{\rho_u\eta_k}\,\mathbb{E}\left\{\sum_{m=1}^{M}\alpha_{mk}g_{mk}\hat{g}_{mk}^*\right\}, \tag{8}$$

$$\mathrm{BU}_k \triangleq \rho_u\eta_k\,\mathbb{V}\mathrm{ar}\left\{\sum_{m=1}^{M}\alpha_{mk}g_{mk}\hat{g}_{mk}^*\right\}, \tag{9}$$

$$\mathrm{UI}_{kk'} \triangleq \rho_u\eta_{k'}\,\mathbb{E}\left\{\left|\sum_{m=1}^{M}\alpha_{mk}\hat{g}_{mk}^*g_{mk'}\right|^2\right\}, \tag{10}$$

$$\mathrm{AN}_k \triangleq \mathbb{E}\left\{\left|\sum_{m=1}^{M}\alpha_{mk}\hat{g}_{mk}^*w_{\mathrm{u},m}\right|^2\right\}. \tag{11}$$

Using a similar methodology as in [7], we obtain the following rigorous closed–form expression for the spectral efficiency of the k–th UE:

$$R_k = \frac{\tau_{\rm c} - \tau_{\rm p}}{\tau_{\rm c}} \log_2\left(1 + {\rm SINR}_k\right),\qquad(12)$$

where, ${\rm SINR}_k$ represents the uplink SINR, given by

$${\rm SINR}_k = \qquad\qquad\qquad\qquad\qquad\qquad(13)$$

$$\frac{\rho_{\rm u}\eta_k \left|\mathbf{a}_k^H \bar{\boldsymbol{\gamma}}_k\right|^2}{\rho_{\rm u}\sum_{k'=1}^K \eta_{k'}\xi_{kk'} + \rho_{\rm u}\sum_{k'\neq k}^K \eta_{k'}\omega_{kk'}\left|\boldsymbol{\varphi}_k^H\boldsymbol{\varphi}_{k'}\right|^2 + \mathbf{a}_k^H\bar{\boldsymbol{\Gamma}}_k\mathbf{a}_k}.$$

In (13), $\mathbf{a}_k = [\alpha_{1k},\ldots,\alpha_{Mk}]^T$, $\bar{\boldsymbol{\gamma}}_k = [\bar{\gamma}_{1k},\ldots,\bar{\gamma}_{Mk}]$, $\bar{\gamma}_{mk} = \gamma_{mk} + |\bar{g}_{mk}|^2$,

$$\xi_{kk'} = \mathbf{a}_k^H \mathbf{R}_{k'}\boldsymbol{\Gamma}_k\mathbf{a}_k + \mathbf{a}_k^H\boldsymbol{\Gamma}_k\bar{\mathbf{G}}_{k'}\mathbf{a}_k + \mathbf{a}_k^H\mathbf{R}_{k'}\bar{\mathbf{G}}_k\mathbf{a}_k$$
$$+ (1-\delta_{kk'})\left|\mathbf{a}_k^H\mathbf{b}_{kk'}\right|^2,\qquad(14)$$

and

$$\omega_{kk'} = \left|\mathbf{a}_k^H\mathbf{d}_{kk'}\right|^2 + 2\mathbf{a}_k^H\mathbf{d}_{kk'}{\rm Re}\left\{\mathbf{a}_k^H\mathbf{b}_{kk'}^*\right\},\qquad(15)$$

where $\delta_{kk'} = 1$ when $k = k'$ and 0 otherwise, $\mathbf{R}_k = {\rm diag}\{\beta_{1k},\ldots,\beta_{Mk}\}$, $\boldsymbol{\Gamma}_k = {\rm diag}\{\gamma_{1k},\ldots,\gamma_{Mk}\}$, $\bar{\mathbf{G}}_k = {\rm diag}\{|\bar{g}_{1k}|^2,\ldots,|\bar{g}_{Mk}|^2\}$, $\mathbf{b}_{kk'} = [\bar{g}_{1k}^*\bar{g}_{1k'},\ldots,\bar{g}_{Mk}^*\bar{g}_{Mk'}]$, $\mathbf{d}_{kk'} = \left[\gamma_{1k}\frac{\beta_{1k'}}{\beta_{1k}},\ldots,\gamma_{Mk}\frac{\beta_{Mk'}}{\beta_{Mk}}\right]^T$, and $\bar{\boldsymbol{\Gamma}}_k \triangleq {\rm diag}\{\bar{\gamma}_{1k},\ldots,\bar{\gamma}_{Mk}\}$.

Remark 2. Similar to the case of uncorrelated Rayleigh fading channels, the performance of cell–free massive MIMO is limited by the pilot contamination since the second term of the denominator in (13) scales with the same rate as the numerator (i.e. with M^2) when M increases. To see the effect of the LOS components, we consider a simple scenario where $\alpha_{mk} = 1$, and $\boldsymbol{\varphi}_k^H\boldsymbol{\varphi}_{k'} = 0$, for $k \neq k'$. The inter–user interference term can be rewritten as

$$\xi_{kk'} = \sum_{m=1}^M \left(\beta_{mk'}\gamma_{mk} + \gamma_{mk}|\bar{g}_{mk'}|^2 + \beta_{mk'}|\bar{g}_{mk}|^2\right)$$
$$+ (1-\delta_{kk'})\left|\sum_{m=1}^M \bar{g}_{mk}^*\bar{g}_{mk'}\right|^2.\qquad(16)$$

If $\omega_{mk'} = \omega_{mk} + n\pi$, where n is an integer, then

$$\bar{g}_{mk}^*\bar{g}_{mk'} = \frac{\zeta_{mk}K_{mk}\zeta_{mk'}K_{mk'}}{(K_{mk}+1)(K_{mk'}+1)}e^{j(\omega_{mk'}-\omega_{mk})}$$
$$= \frac{\zeta_{mk}K_{mk}\zeta_{mk'}K_{mk'}}{(K_{mk}+1)(K_{mk'}+1)}.\qquad(17)$$

As a result, the last term of (16) scales as M^2 when M increases. The spectral efficiency is upper-bounded by a finite value when M goes to infinity. This implies that, beside the pilot contamination effect, in the case where we have strong alignment of two distinct LOS responses, the inter-user interference persists even when M is infinity. To reduce this effect, user scheduling and power control need to be done.

IV. RESOURCE ALLOCATION

A. Max-Min Power and AP-Weighting coefficient Control

In this section, we investigate an optimization problem which selects the power coefficients $\{\eta_k\}$ together with the AP–weighting coefficients $\{\mathbf{a}_k\}$ to maximize the smallest spectral efficiency of all UEs. Mathematically, the max–min power and AP–weighting control problem can be formulated as follows:

$$(\mathcal{P}): \begin{cases} \max_{\{\mathbf{a}_k,\eta_k\}} & \min_{k=1,\cdots,K} R_k \\ \text{subject to } 0 \leq \eta_k \leq 1,\ k=1,...,K, \\ \qquad\qquad \|\mathbf{a}_k\|^2 \leq 1,\ k=1,...,K. \end{cases}\qquad(18)$$

Since $\log(\cdot)$ is an increasing function, problem $\mathcal{P}$ can be rewritten as

$$(\mathcal{P}): \begin{cases} \max_{\{\mathbf{a}_k,\eta_k\}} & \min_{k=1,\cdots,K} {\rm SINR}_k \\ \text{subject to } 0 \leq \eta_k \leq 1,\ k=1,...,K, \\ \qquad\qquad \|\mathbf{a}_k\|^2 \leq 1,\ k=1,...,K. \end{cases}\qquad(19)$$

Remark 3. Problem $\mathcal{P}$ is *not jointly convex* with respect to $\{\mathbf{a}_k\}$ and $\{\eta_k\}$. However, we will show later that problem $\mathcal{P}$ can be reformulated to convex problem with respect to $\mathbf{a}_k$ (if η_k is fixed) or η_k (if $\mathbf{a}_k$ is fixed). Therefore, we can decouple problem $\mathcal{P}$ into two sub-problems: $(\mathcal{P}_1)$–solving η_k with fixed $\mathbf{a}_k$; and $(\mathcal{P}_2)$-solving $\mathbf{a}_k$ with fixed η_k. These sub–problems are alternately solved to obtain the total solution for $\mathcal{P}$.

1) Problem $\mathcal{P}_1$: Problem $\mathcal{P}_1$ is obtained from $\mathcal{P}$ when $\mathbf{a}_k$ is fixed. Thus, we have

$$(\mathcal{P}_1): \begin{cases} \max_{\{\eta_k\}} & \min_{k=1,\cdots,K} {\rm SINR}_k \\ \text{subject to } 0 \leq \eta_k \leq 1,\ k=1,...,K, \end{cases}\qquad(20)$$

which can be equivalently reformulated as

$$(\mathcal{P}_1): \begin{cases} \max_{t,\{\eta_k\}} & t \\ \text{subject to } t \leq {\rm SINR}_k,\ k=1,...,K, \\ \qquad\qquad 0 \leq \eta_k \leq 1,\ k=1,...,K. \end{cases}\qquad(21)$$

From (13), we have

$$(\mathcal{P}_1): \begin{cases} \max_{t,\{\eta_k\}} t \\ \text{s.t.}\quad \rho_{\rm u}\sum_{k'=1}^K \eta_{k'}\xi_{k'} + \rho_{\rm u}\sum_{k'\neq k}^K \eta_{k'}\omega_{k'}\left|\boldsymbol{\varphi}_k^H\boldsymbol{\varphi}_{k'}\right|^2 \\ +\mathbf{a}_k^H\bar{\boldsymbol{\Gamma}}_k\mathbf{a}_k \leq \frac{1}{t}\rho_{\rm u}\eta_k\left|\mathbf{a}_k^H\bar{\boldsymbol{\gamma}}_k\right|^2,\ k=1,...,K, \\ 0 \leq \eta_k \leq 1,\ k=1,...,K, \end{cases}\qquad(22)$$

For a given t, all inequalities involved in (22) are linear, and hence, the program (22) is quasi–linear. As a consequence, problem (22) can be efficiently solved by using the bisection method and solving a sequence of linear feasibility problems.

2) Problem $\mathcal{P}_2$: The optimization problem $\mathcal{P}_2$ is

$$(\mathcal{P}_2): \begin{cases} \max_{\{\mathbf{a}_k\}} & \min_{k=1,\cdots,K} {\rm SINR}_k \\ \text{subject to } \|\mathbf{a}_k\|^2 \leq 1,\ k=1,...,K. \end{cases}\qquad(23)$$

To solve (23), we rewrite the SINR as follows:

$$\text{SINR}_k =$$

$$\frac{\mathbf{a}_k^H \left(\rho_{\mathrm{u}} \eta_k \bar{\boldsymbol{\gamma}}_k \bar{\boldsymbol{\gamma}}_k^H \right) \mathbf{a}_k}{\mathbf{a}_k^H \left(\rho_{\mathrm{u}} \sum\limits_{k'=1}^{K} \eta_{k'} \boldsymbol{\Lambda}_{kk'} + \rho_{\mathrm{u}} \sum\limits_{k' \neq k}^{K} \eta_{k'} \boldsymbol{\Xi}_{kk'} \left| \boldsymbol{\varphi}_k^H \boldsymbol{\varphi}_{k'} \right|^2 + \bar{\boldsymbol{\Gamma}}_k \right) \mathbf{a}_k},$$

$$(24)$$

where $\boldsymbol{\Lambda}_{kk'} = \mathbf{R}_{k'} \boldsymbol{\Gamma}_k + \boldsymbol{\Gamma}_k \bar{\mathbf{G}}_{k'} + \mathbf{R}_{k'} \bar{\mathbf{G}}_k + (1 - \delta_{kk'}) \mathbf{b}_{kk'} \mathbf{b}_{kk'}^H$, and $\boldsymbol{\Xi}_{kk'} = \mathbf{d}_{kk'} \mathbf{d}_{kk'}^H + 2 \mathbf{d}_{kk'} \text{Re} \{ \mathbf{b}_{kk'} \}^H$.

Remark 4. Since SINR_k depends only on $\mathbf{a}_k$ (does not include $\mathbf{a}_{k'}$ for $k' \neq k$), the solutions of (23) can be obtained by solving K optimization problems, separately. In the k–th problem, we will find $\mathbf{a}_k$ which maximize SINR_k, for $k = 1, \ldots K$. We can see that the SINR_k given by (24) is a generalized Rayleigh quotient whose maximum value is equal to $\lambda_{\max}$, which corresponds to the largest eigenvalue of the generalized eigenvalue problem. The optimal $\mathbf{a}_k$ is the eigenvector corresponding to $\lambda_{\max}$. Note that $\mathbf{a}_k$ has to be normalized so that $\|\mathbf{a}_k\|^2 = 1$.

Combing Problems $\mathcal{P}_1$ and $\mathcal{P}_2$, we can obtain the optimal solution for $\mathcal{P}$ as summarized in Algorithm 1.

Algorithm 1 (Iterative algorithm to solve $\mathcal{P}$):

---

1. *Initialization*: set $n = 1$, choose the initial value of $\mathbf{a}_k$. Define a tolerance ϵ and the maximum number of iterations N_{I}.
2. *Iteration n:*
    - solve (22) using bisection algorithm. Let η_k^* be the solution.
    - set $\eta_k = \eta_k^*$, solve (23) via solving the generalized eigenvalue problem. Let $\mathbf{a}_k^*$ be the solution.
3. If $\left| \sum_{k=1}^{K} \left(t_k^* - t_k^{(n)} \right) \right| < \epsilon$ or $n = N_{\mathrm{I}} \rightarrow$ Stop and set $\mathbf{a}_k^* = \mathbf{a}_k^* / \|\mathbf{a}_k^*\|$. Otherwise, go to step 4.
4. Set $n = n + 1$, update $\mathbf{a}_k = \mathbf{a}_k^*$, go to step 2.

B. AP Selection

To detect the signal transmitted from the k–th UE, all M APs forward the processed signals $\alpha_{mk} \hat{g}_{mk}^* y_{\mathrm{u},m}$, for $m = 1, \ldots, M$, to the CPU via the backhaul. This induces a huge backhaul burden. To reduce this backhaul requirement, we propose a new AP selection scheme where the m–th AP processes and forwards its received signals only if α_{mk} (obtained from Algorithm 1) is greater than a threshold. The details of our proposed AP selection are as follows.

- **Step 1.** Perform Algorithm 1.
- **Step 2.** If $|\alpha_{mk}| \leq \alpha_{\mathrm{th}}$, then set $\alpha_{mk} = 0$. Here α_{th} denotes a pre-defined threshold.
- **Step 3.** With the new $\{\alpha_{mk}\}$ given in Step 2, solve (22) using bisection algorithm. The optimal η_k, for $k = 1, \cdots, K$, will be determined.

V. NUMERICAL RESULTS

We assume that all M APs and K users are located at random in a square of 1×1 m^2. Wrapped-around technique is used to imitate a network with an infinite area. The Ricean K–factors and large–scale fading coefficients vary depending on the *locations* of users and APs. To model this, we use the following formulation as in [10]

$$K_{mk} = \frac{P_{\mathrm{LOS}}(d_{mk})}{1 - P_{\mathrm{LOS}}(d_{mk})}, \quad (25)$$

where d_{mk} is the distance between the m–th AP and the k–th user, $P_{\mathrm{LOS}}(d_{mk})$ is the LOS probability depending on the distance d_{mk}. For the LOS probability, we use the model from the 3GPP–UMa as [11]

$$P_{\mathrm{LOS}}(d_{mk}) = \min\left(\frac{18}{d_{mk}}, 1 \right) \left(1 - e^{-\frac{d_{mk}}{63}} \right) + e^{\frac{-d_{mk}}{63}}, \quad (26)$$

where d_{mk} is in meters. In addition, the large–scale fading coefficient ζ_{mk} is modeled as in [1]. More precisely, large–scale fading is the product of the geometric attenuation with shadow fading. The attenuation follows the three–slope model and the shadowing follows log–normal distribution. In addition, the attenuation and shadow fading also depend on the LOS probability in (26).

A. Parameters and Setup

Most of the network parameters are the same as the ones in [1]: $\tau_{\mathrm{c}} = 200$, $\tau_{\mathrm{p}} = 20$, carrier frequency = 1.9 GHz, bandwidth $B = 20$ MHz, noise power $N_0 = -90$ dBm, and $\rho_{\mathrm{p}} = \rho_{\mathrm{u}} = 0.2/N_0$. Furthermore, random pilot assignment is used, and LOS phase ω_{mk} is uniformly distributed between 0 and 2π. To make a strong connection between Ricean and large–scale fading model, the attenuation exponent and shadowing standard deviation are chosen as follows:

- If $d_{mk} > 70$ m (which corresponds to $P_{\mathrm{LOS}}(d_{mk}) < 0.5$), the attenuation exponent is 3.5, and shadowing standard deviation is 8 dB.
- If $1 < d_{mk} \leq 70$ m (which corresponds to $P_{\mathrm{LOS}}(d_{mk}) \geq 0.5$) the attenuation exponent is 2, and shadowing standard deviation is 3 dB [12].
- If $d_{mk} \leq 1$ m, the attenuation exponent is 0, and there is no shadowing, since the propagating wavefront is in transition from near to far–field.

B. Results and Discussions

We consider the per–UE throughput which takes into account the channel estimation overhead and the system bandwidth, defined as $S_k = B \times R_k$ (bit/s). From our numerical results (were not shown here), Algorithm 1 converges very fast, within about 2 or 3 iterations. Thus, hereafter we choose $N_{\mathrm{I}} = 3$ for Algorithm 1.

First, we examine the effectiveness of using power and AP–weighting coefficient control provided in Algorithm 1 as well as the AP selection scheme proposed in Section IV-B. Figure 1 shows the cumulative distribution of the per–user throughput for four cases: full power and AP–weighting
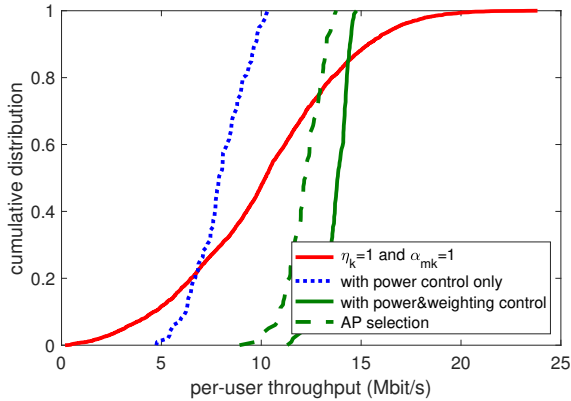
Fig. 1. Cumulative distribution of the per-user throughput. Here $M = 100$, $K = 40$, and $\tau_{\mathrm{p}} = 20$.

Fig. 2. Per-user throughput versus the backhaul usage. Here $K = 40$, $D = 1$ km, and $\tau_{\mathrm{p}} = 20$.

coefficients ($\eta_k = 1$ and $\alpha_{mk} = 1$), optimal power control but no optimal weighting coefficient control ($\alpha_{mk} = 1$, η_k is optimally chosen), optimal power and AP–weighting coefficient control (Algorithm 1), and optimal power and AP–weighting coefficients with AP selection. For the AP selection scheme, we choose $\alpha_{\mathrm{th}} = 1/M$. We can see that max–min power and AP–weighting control improves the system performance significantly. In particular, compared with the case where $\eta_k = 1$ and $\alpha_{mk} = 1$, the power control can improve the 95%–likely per–UE throughput by a factor of 3, while the power control together with the AP–weighting control can improve the 95%-likely per–UE throughput by a factor of 5.4. In addition, we can see that with our proposed AP selection scheme, the throughput is slightly reduced compared to the case without AP selection. But the backhaul requirement reduces noticeably. From the numerical results, on average only about 70 (over 100) APs need to forward the processed signals to the CPU.

To further see the benefit of our AP selection scheme, we plot the per–user throughput as the function of the backhaul usage. The backhaul usage is defined as $\mathrm{BU} = \frac{\sum_{k=1}^{K} M_k}{MK} \times 100\%$, where M_k is the number of selected APs which used to detect q_k. See Figure 2 with $K = 40$, and different M, for one snapshot of the large-scale fading realization. We can see that our proposed AP selection scheme reduces the backhaul requirements substantially with small reduction in performance. In particular, with our AP selection scheme, we need only about 60% and 75% backhaul usages for $M = 200$ and $M = 100$, respectively, to obtain 85% the throughput where all APs are used. Finally, we compare the performance of cell–free massive MIMO with Rayleigh and Ricean channels. For Rayleigh fading, we use the results in [1]. Figure 3 shows the cumulative distribution of per–UE throughput under Rayleigh and Ricean channels for different K. Here, max–min power and AP–weighting control is taken into account. The Ricean channel offers better throughput than Rayleigh channel does.
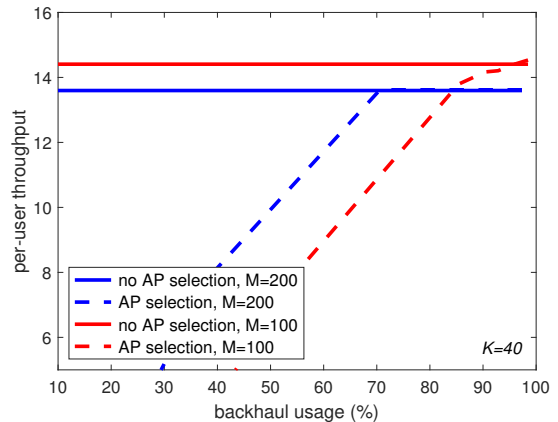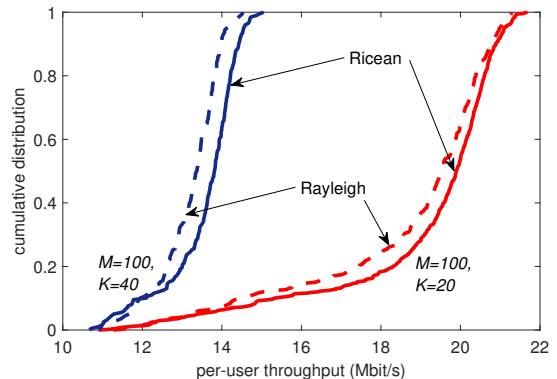

Fig. 3. Cumulative distribution of the per-user throughput for Rayleigh and Ricean channels, with max-min power and AP-weighting control.

VI. CONCLUSION

This paper considered a TDD cell-free massive MIMO system under Ricean channels which include a LOS component plus a non-LOS component. The Ricean K–factor of each link varies with the UE and AP locations. The LOS phases were assumed to be known a priori. The performance of this system with imperfect channel estimation is analyzed in terms of per-user spectral throughput. In particular, simple max-min power and AP–weighting control together with AP selection algorithms were proposed to improve the system performance. The results showed that the proposed algorithms improve the user throughput and reduce the backhaul requirements in cell-free massive MIMO significantly. Future work may include studying the scenarios where the LOS phases are unknown. We hypothesize that these scenarios are more realistic since the phases change very quickly and are hard to be estimated.

REFERENCES

[1] H. Q. Ngo, A. Ashikhmin, H. Yang, E. G. Larsson, and T. L. Marzetta, "Cell-free massive MIMO versus small cells," *IEEE Trans. Wireless Commun.*, vol. 16, no. 3, pp. 1834-1850, Mar. 2017.

[2] S. Buzzi and C. DAndrea, "Cell-free massive MIMO: User-centric approach," *IEEE Wireless Commun. Lett.,* vol. 6, no. 6, pp. 706-709, Dec. 2017.

[3] E. Nayebi, A. Ashikhmin, T. L. Marzetta, B. D. Rao, "Performance of cell-free massive MIMO systems with MMSE and LSFD receivers," in *Proc. IEEE ASILOMAR*, Nov. 2016.

[4] G. Interdonato, E. Björnson, H. Q. Ngo, P. Frenger, and E. G. Larsson, "Ubiquitous cell-free massive MIMO communications," Apr. 2018, Available: [Online]. https://arxiv.org/pdf/1804.03421.pdf.

[5] Z. Chen and E. Björnson, "Channel hardening and favorable propagation in cell-free massive MIMO with stochastic geometry," *IEEE Trans. Commun.*, vol. 66, no. 11, pp. 5205-5219, Nov. 2018.

[6] H. Tataria, P. J. Smith, L. J. Greenstein, and P. A. Dmochowski, "Zero-forcing precoding performance in multiuser MIMO systems with heterogeneous Ricean fading," *IEEE Wireless Commun. Lett.*, vol. 6, no. 1, pp. 74-77, Feb. 2017.

[7] Ö. Özdogan, E. Björnson, and J. Zhang, "Cell-free massive MIMO with Rician fading: Estimation schemes and spectral efficiency," in *Proc. IEEE ASILOMAR*, Nov. 2018.

[8] S. M. Kay, *Fundamentals of Statistical Signal Processing: Estimation Theory*, Prentice Hall, Englewood Cliffs, NJ, 1993.

[9] T. L. Marzetta, E. G. Larsson, H. Yang, and H. Q. Ngo, *Fundamentals of Massive MIMO*, Cambridge University Press, U.K., 2016.

[10] A. H. Jafari, D. López-Pérez, M. Ding, and J. Zhang, "Study on scheduling techniques for ultra dense small cell networks," in *Proc. IEEE VTC-Fall*, Sep. 2015.

[11] I. Rodriguez, *et al.*, "Path loss validation for urban micro cell scenarios at 3.5 GHz compared to 1.9 GHz," *Proc. IEEE GLOBECOM*, Dec. 2013.

[12] 3GPP TR 36.873 v12.0.0, "Study on 3D channel model for LTE," Mar. 2017, Available: [Online] https://portal.3gpp.org.